

Application of Lamellar Nickel Hydroxide Membrane as a Tunable Platform for Ionic Thermoelectric Studies

Raktim Gogoi,^a Arnab Ghosh,^a Priyamjeet Deka,^b K.K.R. Datta,^c Kalyan Raidongia^{a*}

^a Department of Chemistry, Indian Institute of Technology Guwahati, Guwahati, Assam 781039, India. E-mail: k.raidongia@iitg.ernet.in

^b School of Energy Science and Engineering, Indian Institute of Technology Guwahati, Guwahati, Assam 781039, India.

^c Functional Nanomaterials Laboratory, Department of Chemistry, Faculty of Engineering and Technology, SRM Institute of Science and Technology, Kattankulathur 603203, Tamil Nadu, India

Table of Contents

1	Experimental methods:	2
1.1.	Chemical required:	2
2	Membrane fabrication:	2
2.1	Fabrication of Ionic Thermoelectric Devices:	5
2.2	Fabrication of ionic thermopile:	7
2.3	Fabrication of nanofluidic device:	7
3	Characterizations:	8
3.1	Instruments for membrane characterization:	8
3.2	Characterizations of Ni-M	9
3.3	Characterizations of Mg-Aminoclay	9
3.4	Characterizations of Ni-AC-Ms	10
3.5	Thermoelectric experiments of Ni-AC-M and Ni-Cl-M membranes:	12
3.6	Structural characterization of Ni-AC-Cl-Ms:	15
3.7	Thermoelectric characterization of Ni-AC-Cl-Ms:	16
3.8	Characterization of Ni-PSS-M:	19
3.9	Thermopiles of Ni-PSS-M and Ni-AC-Cl-M-29:	20

1 Experimental methods:

1.1. Chemical required: Nickel (II) acetate tetrahydrate ($\text{Ni}(\text{CH}_3\text{CO}_2\text{H})_2 \cdot 4\text{H}_2\text{O}$) and Magnesium chloride (MgCl_2) were purchased from SRL Pvt. Ltd., Liquor Ammonia solution and Poly (4-styrenesuphonic acid) (PSS) were purchased from Sigma-Aldrich, 3-aminopropyltriethoxysilane was purchased from Thermo Fischer Scientific. Ethanol was purchased from Changshu Hongheng Fine Co. Ltd. Poly (4-styrenesuphonic acid) (PSS) were purchased from Sigma Aldrich co. Benzyltriethylammonium chloride, Benzyltriethylammonium bromide and Benzyltriethylammonium hydroxide were purchased Avra Synthesis Pvt. Ltd. Vermiculite clay was purchased from Sigma Aldrich. The copper electrodes were purchased from the local market. Silver paste was purchased from Alfa-Aesar Pvt. Ltd.

2 Membrane fabrication:

1.2.1. Preparation of $\text{Ni}(\text{OH})_2$ nanosheets:

0.35 gm of Nickel (II) acetate tetrahydrate ($\text{Ni}(\text{CH}_3\text{CO}_2\text{H})_2 \cdot 4\text{H}_2\text{O}$) was dissolved in 30 ml DI water and then 670 μl 25% aqueous ammonia was added dropwise to it with continuous stirring. The solution was kept afterwards in stirring for 24 hours. A green precipitation was obtained, which was separated from the solution by centrifugation and washed it for several times with DI water. After that the prepared $\text{Ni}(\text{OH})_2$ were transferred into DI water to prepare a dispersion of concentration 10 mg/ml.

1.2.2. Preparation of $\text{Ni}(\text{OH})_2$ membrane:

$\text{Ni}(\text{OH})_2$ membranes were prepared from as-prepared $\text{Ni}(\text{OH})_2$ dispersion through vacuum filtration. Here, 15 ml of (10 mg/ml) $\text{Ni}(\text{OH})_2$ dispersion was vacuum filtrated using a support of PTFE membrane with pore diameter of 0.1 μm and dried in an ambient atmosphere to get a free-standing $\text{Ni}(\text{OH})_2$ membrane.

1.2.3. Preparation of Mg-Aminoclay:

For the preparation of Mg-Aminoclay 1.68 gm of Magnesium chloride (MgCl_2) was dissolved in 40 gm of ethanol and then 2.6 ml of 3-aminopropyltriethoxysilane was added dropwise with rapid stirring. After that the solution was kept at stirring for 24 hours. Resulting product (white) was separated from the solution by centrifugation and washed with ethanol for several times followed by drying at 40 °C in air.

1.2.4. Preparation of $\text{Ni}(\text{OH})_2$ and Mg-aminoclay composite membrane:

Composite membranes of $\text{Ni}(\text{OH})_2$ and Mg-aminoclay were prepared from the vacuum filtration of the composite mixtures of the same compositions. First, different amount of Mg-aminoclay (30 mg, 50 mg, 100 mg and 200 mg) were mixed with 15 ml of 10 mg/ml $\text{Ni}(\text{OH})_2$ dispersion and were sonicated for 20 minutes. After that the respective composite dispersion were vacuum filtrated using a PTFE support with pore diameter of 100 nm and dried in an ambient atmosphere to get a free-standing membrane.

1.2.5. Preparation of $\text{Ni}(\text{OH})_2$ and Benzyltriethylammonium chloride composite (BTAC) membrane:

To prepare the composite membrane of $\text{Ni}(\text{OH})_2$ and BTAC salt, initially 7 ml of $\text{Ni}(\text{OH})_2$ dispersion (10 mg/ml) was vacuum filtered using a PTFE membrane of pore size 100 nm to form a layer of $\text{Ni}(\text{OH})_2$ nanosheets. On the top of the layer a mixture of 8 ml $\text{Ni}(\text{OH})_2$ dispersion (10 mg/ml) and 200 mg BTAC salt was again vacuum filtered and kept it for drying in an ambient atmosphere to get a free-standing Ni-Cl-M membrane.

1.2.6. Preparation of $\text{Ni}(\text{OH})_2$, Mg-aminoclay and different quaternary ammonium salt composite membranes:

To prepare the composite membranes of $\text{Ni}(\text{OH})_2$, Mg-aminoclay and different quaternary ammonium salt, 15 ml $\text{Ni}(\text{OH})_2$ dispersion (10 mg/ml) 100 mg of Mg-

aminoclay were mixed together and sonicated for 20 minutes. Then this dispersion was divided into two equal portions and definite amount of Benzyltriethylammonium chloride (BTAC) (100 mg, 150 mg, 200 mg and 250 mg) were mixed with one of the two portions. The other part without salt (in this part only Ni(OH)₂ and Mg-aminoclay are present) was first vacuum filtered through a 0.1 µm pore diameter PTFE membrane and after near completion of the filtration process, the other fraction containing salt was poured upon it and again vacuum filtered and dried to obtain a free-standing composite membrane. It is worth to mention that, during vacuum filtration all of the BTAC salt will not remain within the Ni(OH)₂ membrane. Based on the ion chromatography experiments of Cl⁻ ions, nearly, ~30 % of the BTAC salts were found to retain within the composite membrane based on which all the weight % of the BTAC salts have been calculated. Following the same procedure, the composite membranes of Ni(OH)₂ (150 mg), Mg-aminoclay (100 mg), Benzyltriethylammonium bromide (200 mg) and Ni(OH)₂ (150 mg), Mg-aminoclay (100 mg), Benzyltriethylammonium hydroxide (200 mg) were prepared.

1.2.7. Preparation of Ni(OH)₂ and Poly(4-styrenesulfonic) acid composite membrane:

For the preparation of Ni(OH)₂ and Poly(4-styrenesulfonic acid) composite membranes, 15 ml (10 mg/ml) of Ni(OH)₂ dispersion was mixed with 1 ml of Poly(4-styrene sulfonic) acid solution (M_w ~75,000) and sonicated for 30 minutes. The resulted composite mixture was vacuum filtrated through PTFE support with the pore diameter of 100 nm and dried in an ambient atmosphere to obtain a free-standing membrane.

1.2.8. Preparation of vermiculite nanosheets and membrane fabrication:

Typically, bulk vermiculite clay was exfoliated through ion exchange method. 200 mg of vermiculite was refluxed at boiling temperature with a saturated aqueous solution of NaCl solution for 24 hours and washed several times with DI water. The Na-exchanged washed sample were then refluxed with 2M of aqueous LiCl solution at boiling temperature for 24 hours followed by washing with DI water. After completion of the washing process, an aqueous dispersion of 1mg/ml concentration was prepared with the washed product.

The free-standing vermiculite membrane were prepared through the vacuum filtration of 40 ml (1mg/ml) vermiculite dispersion through a PTFE membrane with pore diameter of 100 nm. After drying at ambient atmosphere, the vermiculite membrane was peeled off from the support to obtain the free-standing vermiculite membrane.

2.1 Fabrication of Ionic Thermoelectric Devices:

A specific dimension (2 cm x 0.8 cm) of the respective membranes were cut and placed over a stage made of two glass slides with the dimension of 2cm x 2cm. The glass slides were connected together with an adhesive tape and thereby maintaining an air gap of around 2 mm to avoid unwanted heat transfer. The membranes for the measurements were connected with two copper electrodes using conductive silver paste by maintaining a distance of 1.5 cm.

This fabricated thermoelectric device was placed over a stage made of two Peltier devices one of which serves as heat source and the other one as heat sink. The applied temperature difference across the membrane was measured by placing two K-type thermocouples with Testo 735 temperature measuring instrument on the glass slides next to the samples. DC regulated power supply (METARAVI TM – RPS 30005) was

used to power the Peltier devices and therefore to maintain the temperature gradient and the generated thermovoltages were measured using 2450 Keithley Sourcemeter.

All the possible precautions were taken to minimise the possible errors in temperature measurements. The magnitude of probable errors related to the position of temperature measurements were estimated by simultaneously measuring temperature of the glass slides and surface of the samples, with systematically varying the temperature between 18 °C and 35 °C, see plots in Figure S1a and S1b. Typically, the temperature of sample surface was found to be $\sim 1 \pm 0.3$ °C less than the glass surface when the temperature of the glass surface is more than the ambient temperature (~ 23 °C) and $\sim 0.8 \pm 0.4$ °C more than the glass surface when the temperature of the glass surface is less than the ambient temperature (Figure S1a). Similarly, the ΔT values measured between hot and cold zone of sample surface was found to be around $\sim 1.9 \pm 0.5$ °C less than the one measured on the glass surface (Figure S1b).

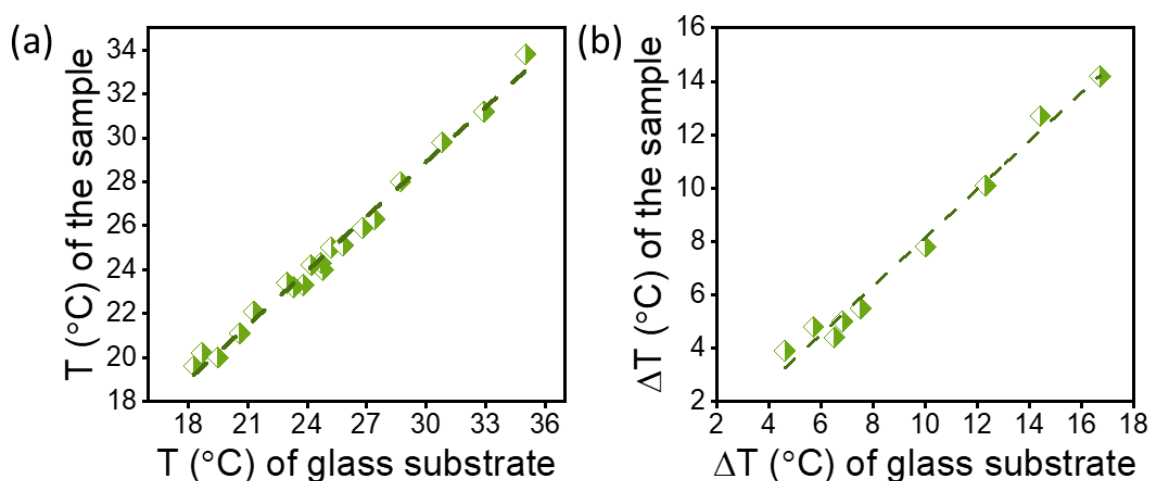


Figure S1: (a) Calibration curve for the temperature of the glass surface and temperature of the sample surface with respect to the glass surface. (b) Calibration curve for the temperature gradient in between the glass surfaces and temperature gradient across sample surface with respect to the glass surface temperature (schematic shown in Figure 2a).

2.2 Fabrication of ionic thermopile:

The ionic thermopile was fabricated through the series connection of Ni-PSS-M and Ni-AC-Cl-M-29 membrane (2cm x 0.8 cm) over a stage made of two glass slides. An air gap was maintained in between two glass slides to avoid unwanted heat transfer.

To draw the additional power, the thermopile was fabricated in such a way that one side of the both Ni-PSS-M and Ni-AC-Cl-M-29 membranes (2cm x 0.8 cm) were connected with a vermiculite membrane (2cm x 0.8 cm). Both of these Ni-PSS-M and Ni-AC-Cl-M-29 membranes were fused with vermiculite membrane by inserting a water droplet of around 20 μ l and letting it dried in an ambient atmosphere. After completion of the drying process one electrode was connected towards the junction of Ni-PSS-M and vermiculite through conductive silver paste and the other electrode was connected towards the junction of Ni-AC-Cl-M-29 and vermiculite.

To main thermopile with the nanofluidic vermiculite membrane is fabricated in the same way as described above, except the two electrodes are connected towards the other side of the vermiculite membrane, one is on the top or the Ni-AC-Cl-M-29 and the other in on the top of the Ni-PSS-M (inset of Figure 6h).

2.3 Fabrication of nanofluidic device:

For the fabrication of the nanofluidic device a rectangular piece of the Ni-M (1.5cm x 0.5cm x 0.005cm) and Ni-AC-M (1.5cm x 0.5cm x 0.0065cm) were encapsulated inside a PDMS elastomer. Then two reservoirs for DI water and electrolyte were curved out from the both end of the nanofluidic device such that the DI water and the electrolyte inside the reservoirs can touch the membranes. The respective membranes were hydrated by keeping the same with DI water filled reservoirs for a period of 12 hours. After completion of the hydrating process ~0.3 ml of NaOH electrolyte with

particular concentration (10^{-6} M to 1 M) were kept inside the reservoirs for a period of ~ 6 hours so that the membranes get sufficient amount of time to soak the respective electrolytes. After completion of the soaking process the I-V curves were taken for that particular concentration of NaOH electrolyte and continued the same procedure for other concentration of NaOH electrolyte as well.

3 Characterizations:

3.1 Instruments for membrane characterization:

- The morphological structures of Ni(OH)₂ membranes were characterized by field emission scanning electron microscope (FESEM) (Zeiss, model: Sigma)
- The nanosheets of Ni(OH)₂ and Mg-Aminoclay were characterized by Field Emission Transmission Electron Microscope (FETEM) (JEOL, Model: 2100F)
- The compositional study was carried out through Energy-dispersive X-ray analysis using field emission scanning electron microscope (FESEM) (Zeiss, model: Sigma)
- The X-ray diffraction pattern were studying by using a Bruker D-205505 Cu-K α radiation ($\lambda = 1.54 \text{ \AA}$) (Rigaku, model: Micromax-007HF).
- IR spectroscopic analysis were carried out in Perkin Elmer (Spectrum Two).
The zeta potential measurements for the aqueous dispersion of nanosheets were measured with Zetasizer instrument (Malvern, Nano-ZS90).

3.2 Characterizations of Ni-M

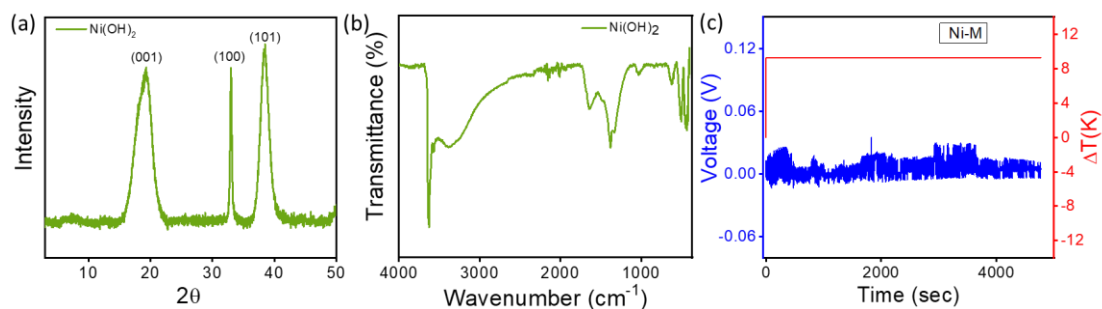


Figure S2: (a) pXRD pattern, and (b) FT-IR spectra for Ni-M membrane (c) negligible response of Ni-M for the temperature gradient of 9 K.

3.3 Characterizations of Mg-Aminoclay

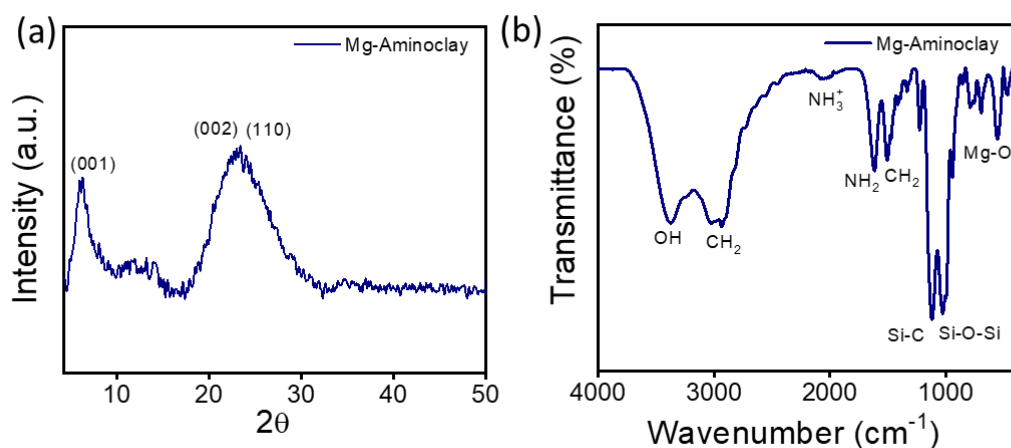


Figure S3: (a) pXRD pattern, and (b) FT-IR spectra of Mg-Aminoclay.

3.4 Characterizations of Ni-AC-Ms

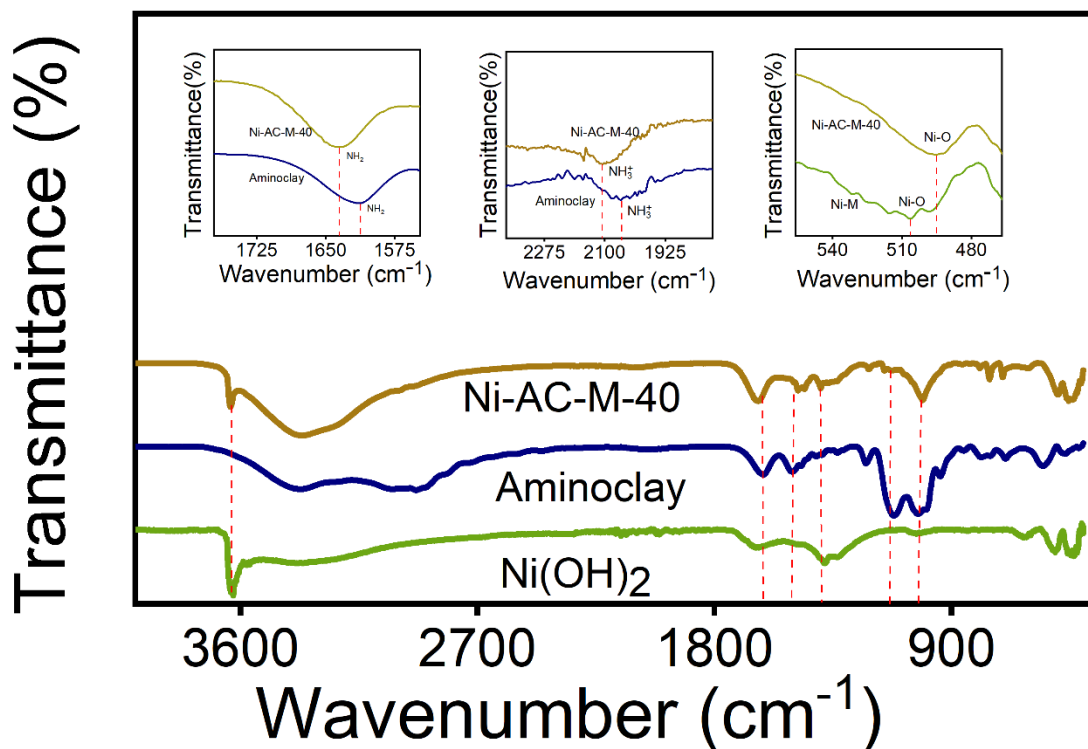


Figure S4: FT-IR spectra of Ni(OH)₂, Mg-Aminoclay and Ni-AC-M-40 membrane, (the inset IR spectra represents the shifts for IR peak positions for respective stretching and bending frequencies)

The FT-IR spectrum of Ni-AC-M is compared with that of β -Ni(OH)₂ and aminoclay. Careful observations of the peak positions attributed to NH₃⁺ stretching and -NH₂ bending reveals shifting from 2050 cm⁻¹ to 2108 cm⁻¹, and 1611 cm⁻¹ to 1635 cm⁻¹, respectively for aminoclay and Ni-AC-M-40 membrane (Inset of Supporting Figure S3). The stretching frequencies of Ni-O for both Ni-M and N-AC-M-40 membrane, shown a downward shift from 506 cm⁻¹ to 495 cm⁻¹, which suggest chemical interactions between -NH₂ groups of aminoclay with Ni²⁺ centres of Ni(OH)₂. Moreover, the IR peaks for the hydrogen bonded and non-hydrogen bonded -OH stretching could be easily observed from the FT-IR spectra of Ni(OH)₂ at 3374 cm⁻¹ and 3631 cm⁻¹. However, the intensity of the IR peak for hydrogen bonded -OH groups was found

to have a higher magnitude in case of N-AC-M-40 membrane as compared to Ni-M whereas, the intensity for non-hydrogen bonded –OH group diminishes, it signifies the existence of hydrogen bonding in between –OH groups in β -Ni(OH)₂ with –NH₂ groups of aminoclay.

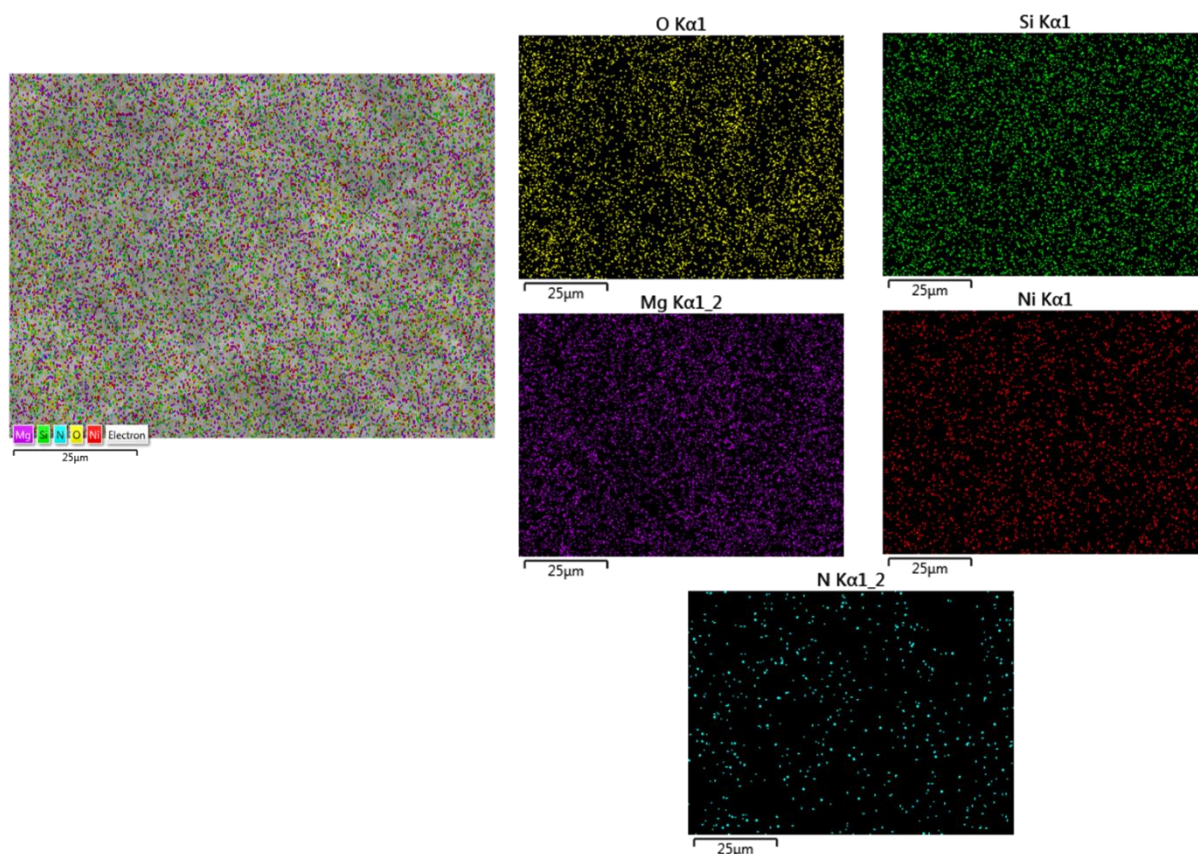


Figure S5: EDX mapping for the composite membrane Ni-AC-M-40.

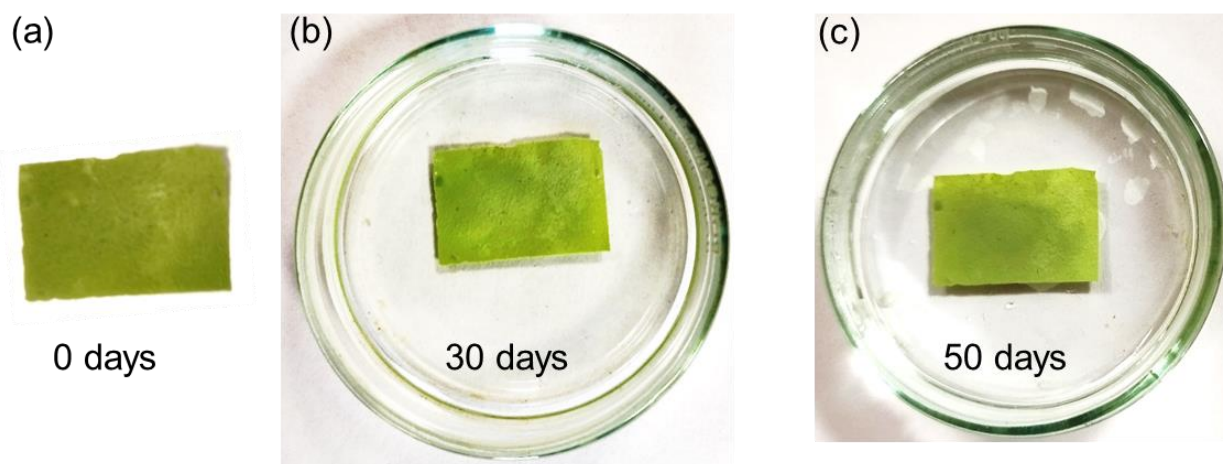


Figure S6: Digital photograph of the Ni-AC-M-40 membrane (a) before soaking in DI water, (b) after 30 days of soaking in DI water, (c) after 50 days of soaking in DI water.

3.5 Thermoelectric experiments of Ni-AC-M and Ni-Cl-M membranes:

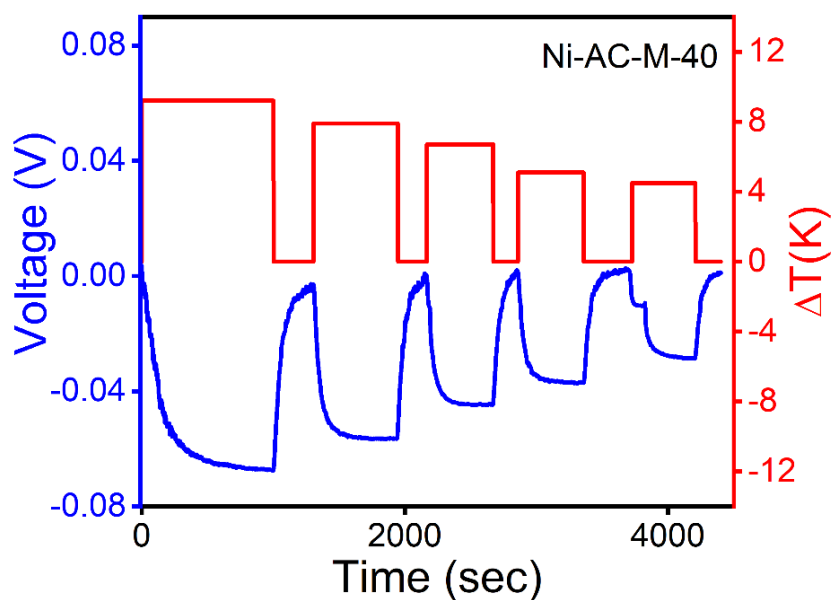


Figure S7: Increment of the ionic thermovoltage with the increase of temperature gradient across Ni-AC-M-40.

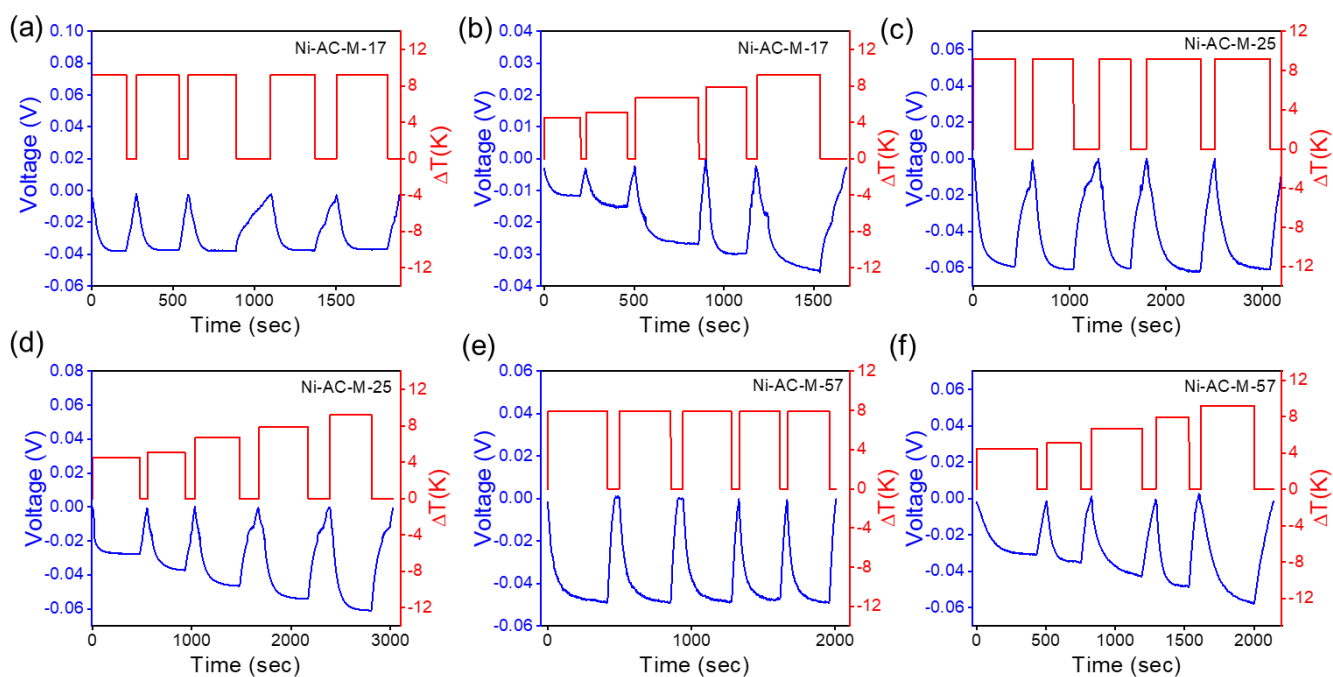


Figure S8: Generation of the thermovoltages by different Ni-AC-Ms

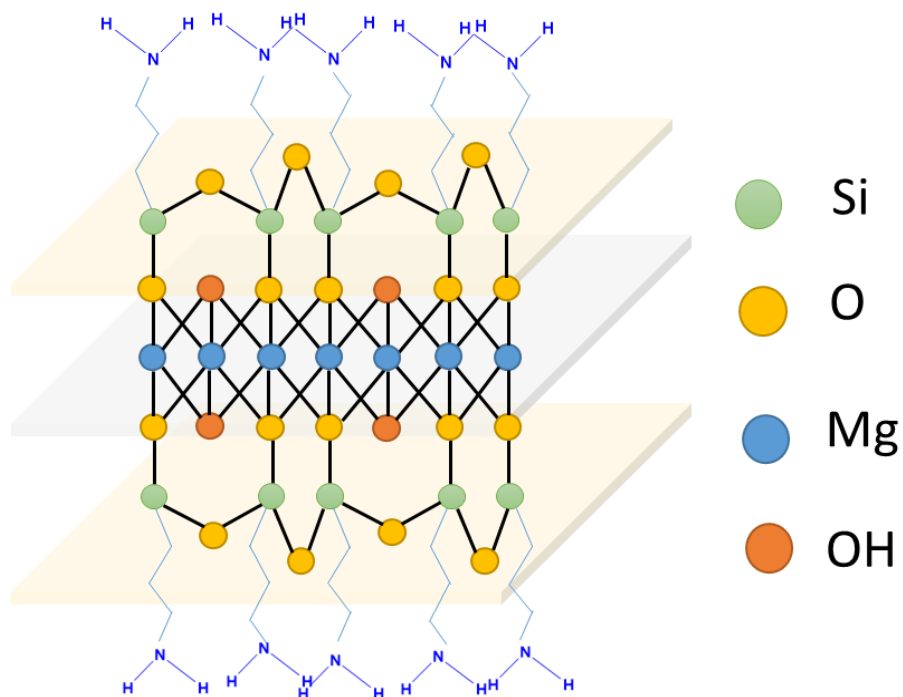


Figure S9: Schematic of the structure of aminoclay.

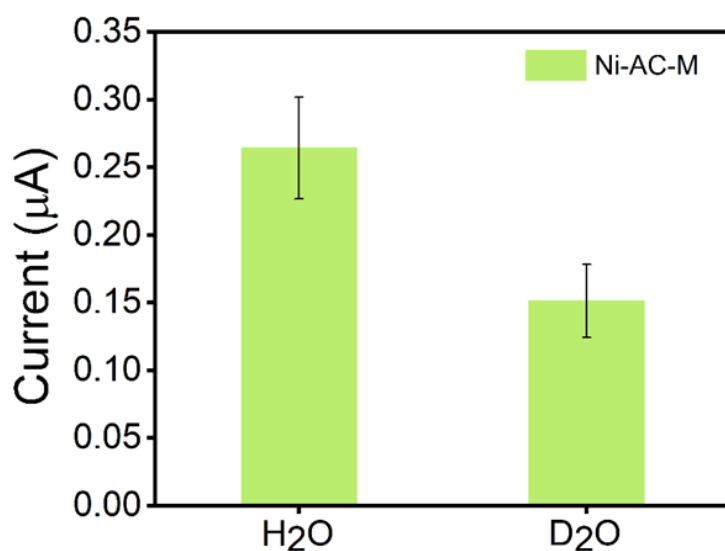


Figure S10: Comparison of the thermal current of Ni-AC-M-40 with H₂O and D₂O under a temperature gradient of 12 K.

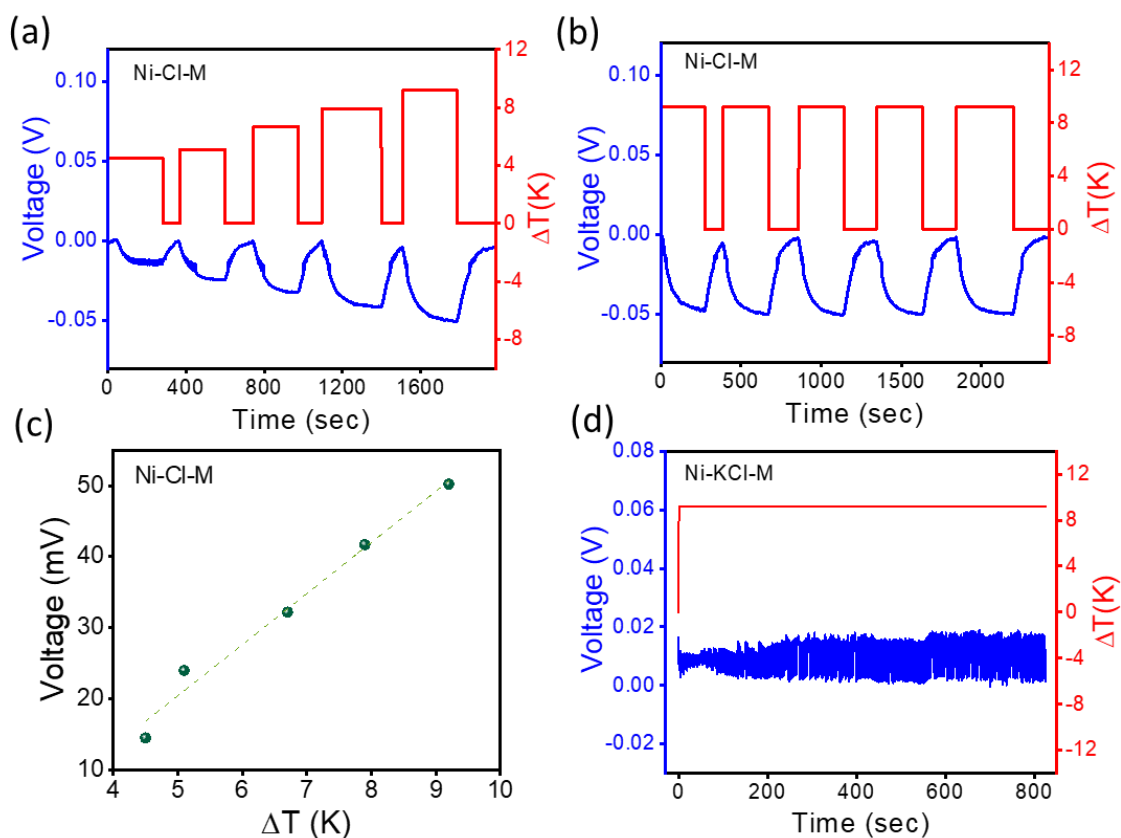


Figure S11: Generation of thermovoltage for Ni-Cl-M membrane (a) at varying temperature gradient (b) at constant temperature gradient. (c) Linear increment of the thermovoltage with respect to temperature gradient (d) negligible response with the temperature gradient across the Ni-KCl-M.

3.6 Structural characterization of Ni-AC-Cl-Ms:

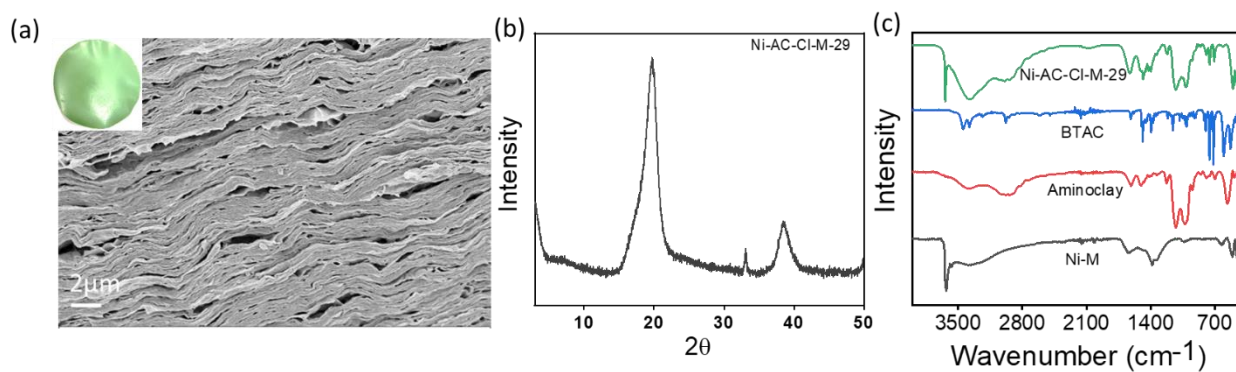


Figure S12: (a) Cross-sectional FESEM image of Ni-AC-Cl-M-29, the inset shows a digital photograph. (b) pXRD pattern, and (c) FT-IR spectra of Ni-AC-Cl-M-29.

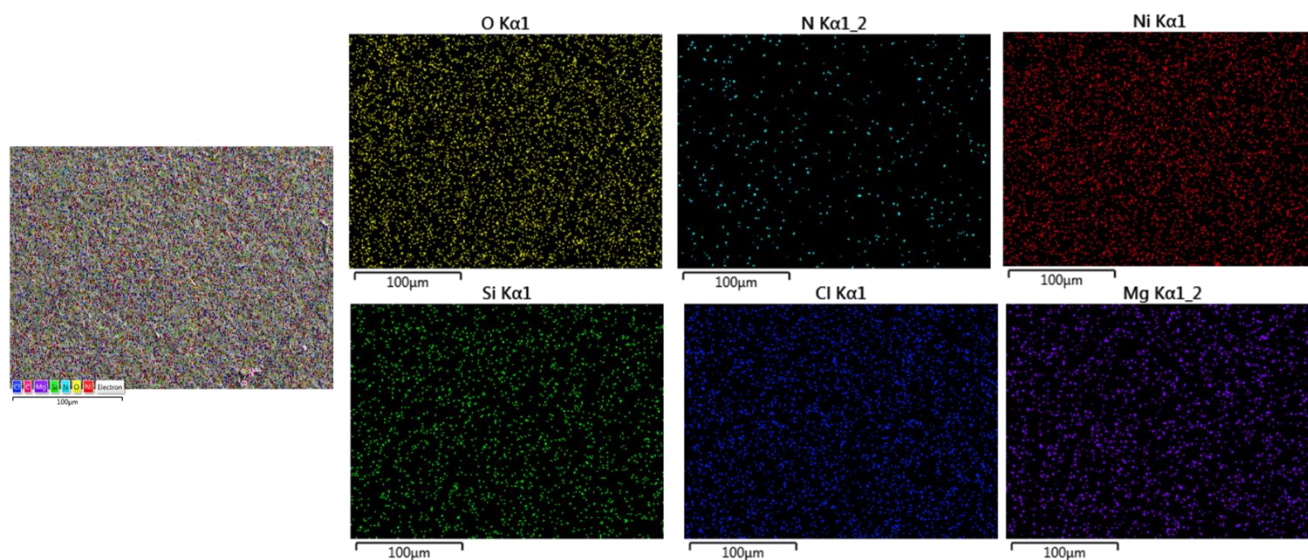


Figure S13: EDX mapping of Ni-AC-Cl-M-29 showing the homogenous distribution of all the elements.

3.7 Thermoelectric characterization of Ni-AC-Cl-Ms:

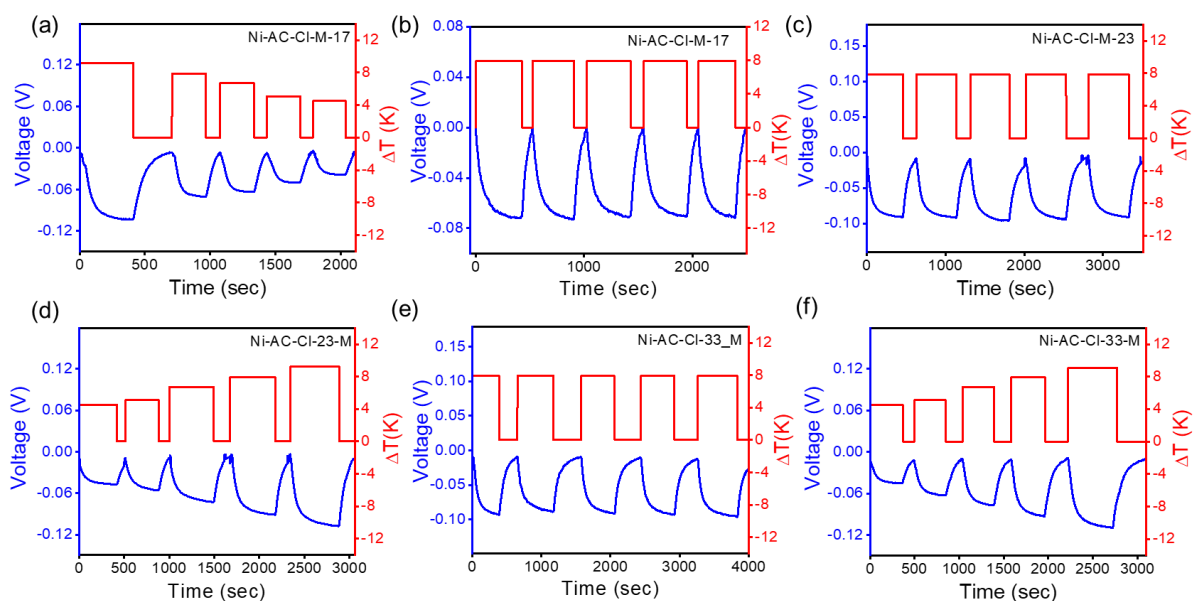


Figure S14: Generation of themovoltages for different composites of Ni-AC-Cl-Ms.

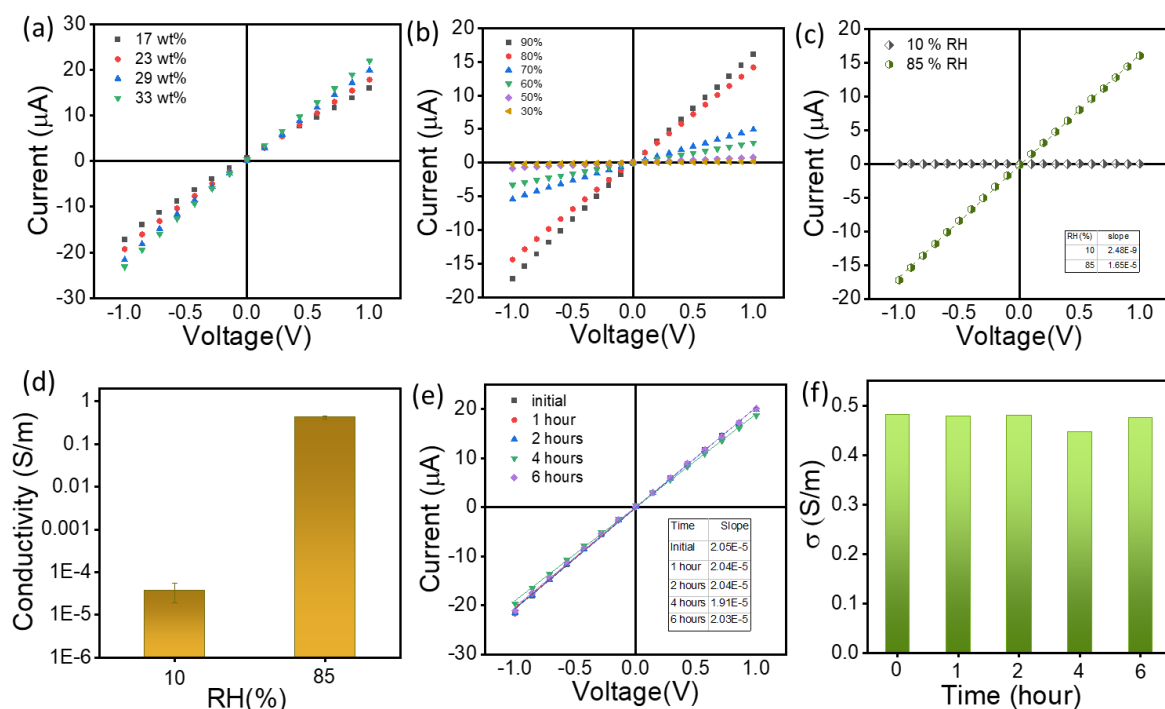


Figure S15: I-V curve of (a) different Ni-AC-Cl-Ms (with varying the wt% of BTAC salt), (b) Ni-AC-Cl-M-29 at different humidity levels, (c) Ni-AC-Cl-M-29 at 10% and 85% RH, (e) AC-Cl-M-29 at different intervals of time. Ionic conductivity values of Ni-AC-Cl-M-29 (d) at 10% and 85% RH, (f) at different intervals of time.

To measure the ionic conductivity values, rectangularly cut pieces of the membrane (2 cm x 0.8 cm) was connected with two copper electrodes with a distance of 1.5 cm apart using conducting silver paste. The electrodes were then connected with the sourcemeter to measure the I-V curves, as shown in Figure S15. The conductivity (σ) was calculated from the slopes of the respective I-V curves using the equation shown below (following the existing literatures^{1,2}).

$$\sigma = \text{slope} \times L/A \quad \dots\dots\dots (1)$$

where,

L = length between the two electrodes

A = cross-sectional area of the membrane

To understand the nature of the conductivity (ionic or electronic), the I-V curves were recorded at varying relative humidity levels (RH % = 85 % and 10 %), shown in Figure S15c. The drastic drop in the conductivity value (from 0.42 ± 0.03 S/m to $3.75 \times 10^{-5} \pm 1.8 \times 10^{-5}$) at lower humidity level indicates that ionic movements is the origin of the obtained conductivity (Figure S15d) as at lower humidity level the movement of ions are restricted due to the absence of water pathways^{3,4}. Further, to find out the time dependency of ionic conductivity the I-V curves were recorded for different intervals of time (Figure S15e) and plotted in Figure S15f concluding a near constant value with time.

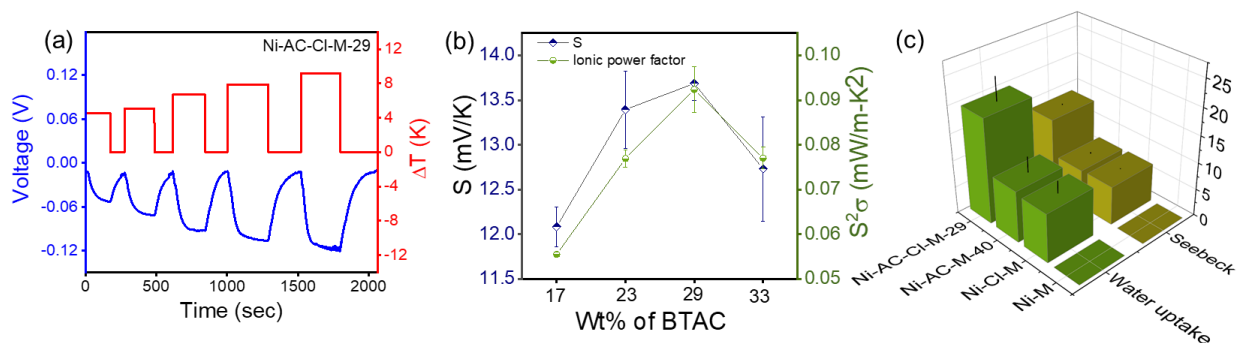


Figure S16: (a) Generation of thermovoltage of Ni-AC-Cl-M-29 at variable temperature gradient. (b) Seebeck coefficients and ionic power factor of different Ni-AC-Cl-Ms (with varying the wt% of BTAC salt). (c) The concordant increment of Seebeck coefficient for Ni-M, Ni-Cl-M, Ni-AC-M-40 and Ni-AC-Cl-M-29 membrane with the water uptake capacity.

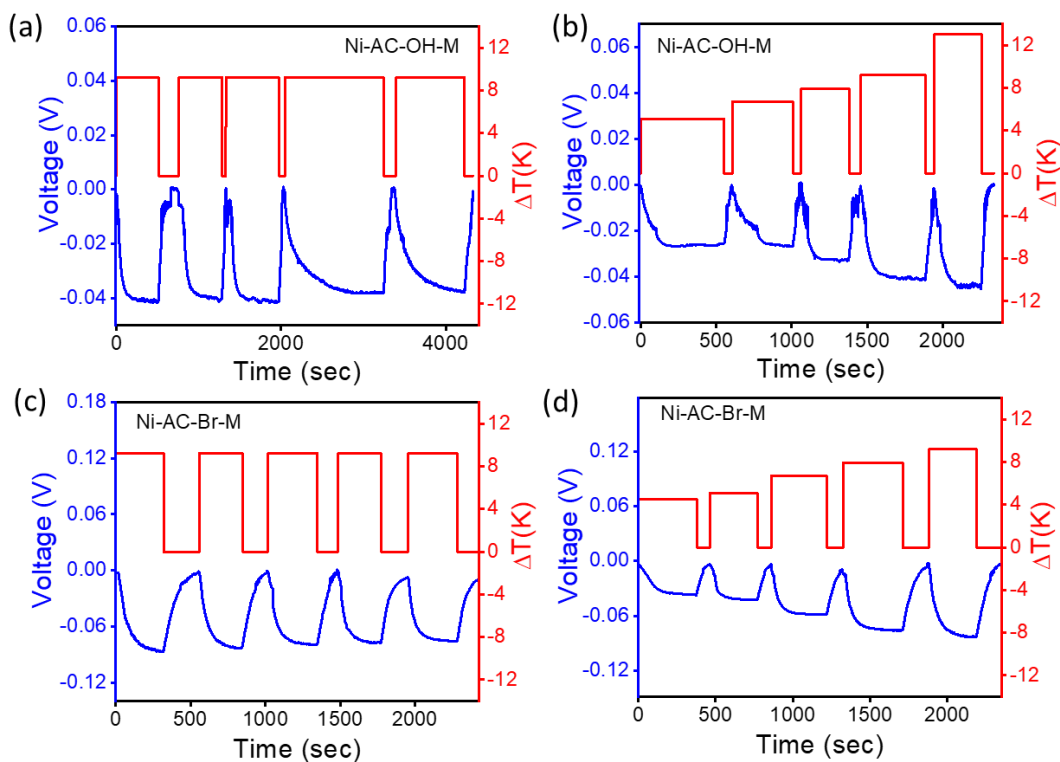


Figure S17: Thermovoltage of Ni-AC-OH-M (a) at constant temperature gradient, and (b) at variable temperature gradient. Thermovoltage of Ni-AC-Br-M (c) at constant temperature gradient, and (d) at variable temperature gradient

3.8 Characterization of Ni-PSS-M:

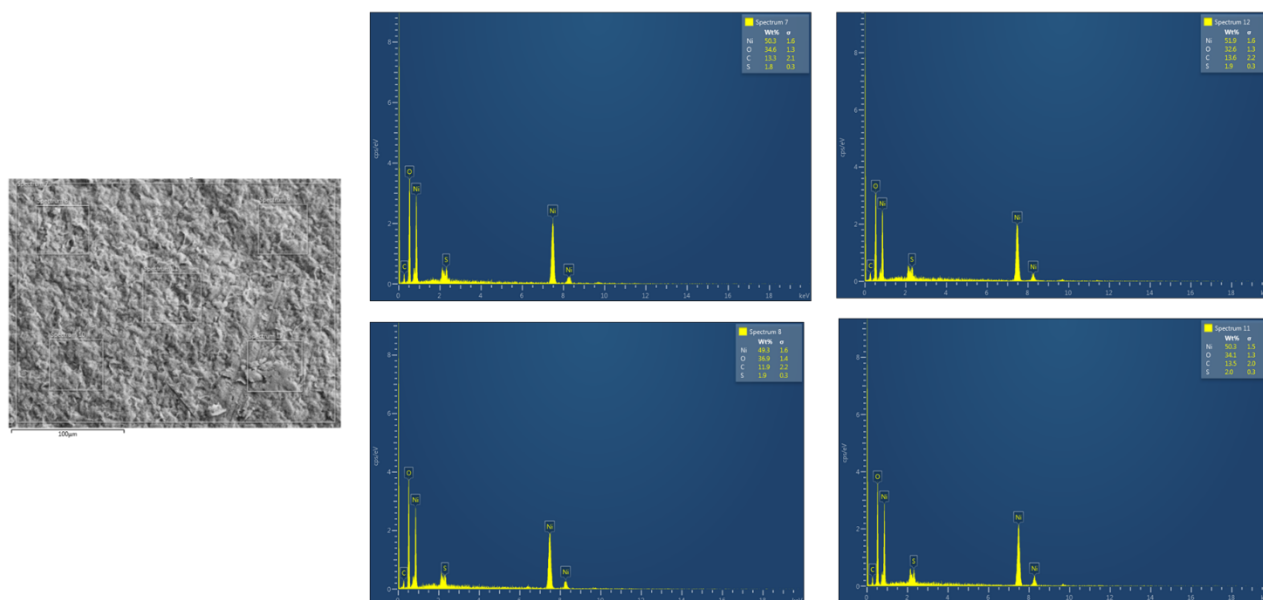


Figure S18: EDX analysis for the Wt% of the elements present in Ni-PSS-M.

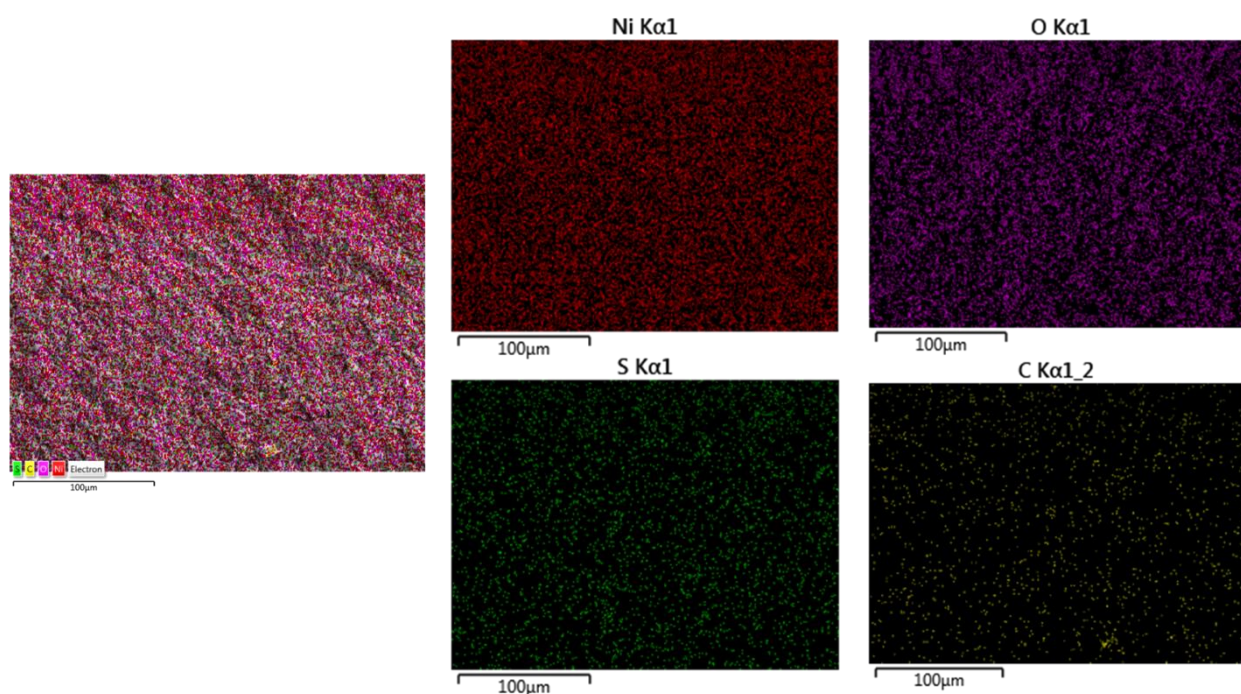


Figure S19: EDX mapping of the elements for Ni-PSS-M showing homogenous distribution of PSS molecules.

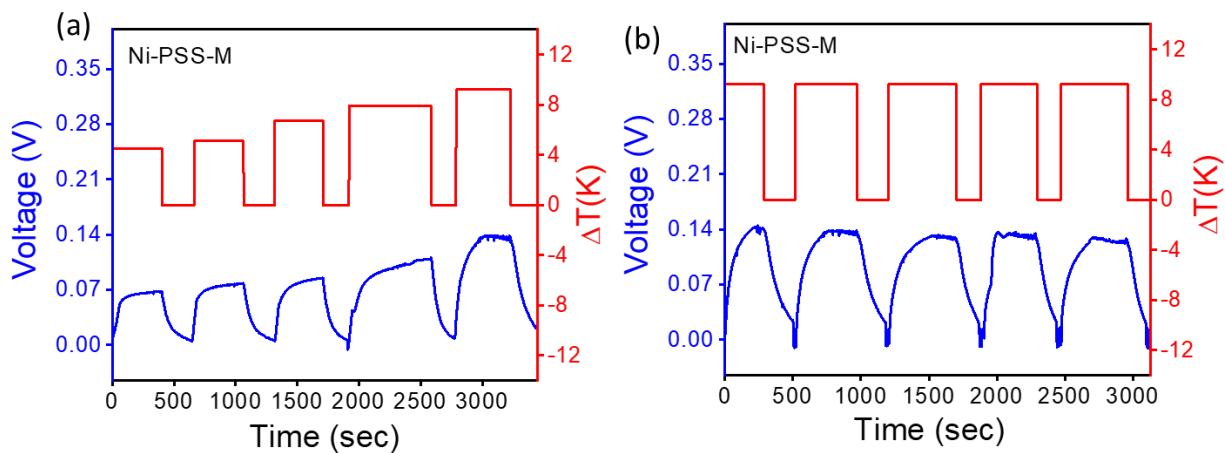


Figure S20: Generation of thermovoltage for Ni-PSS-M membrane (a) at variable temperature gradient and (b) at constant temperature gradient.

3.9 Thermopiles of Ni-PSS-M and Ni-AC-Cl-M-29:

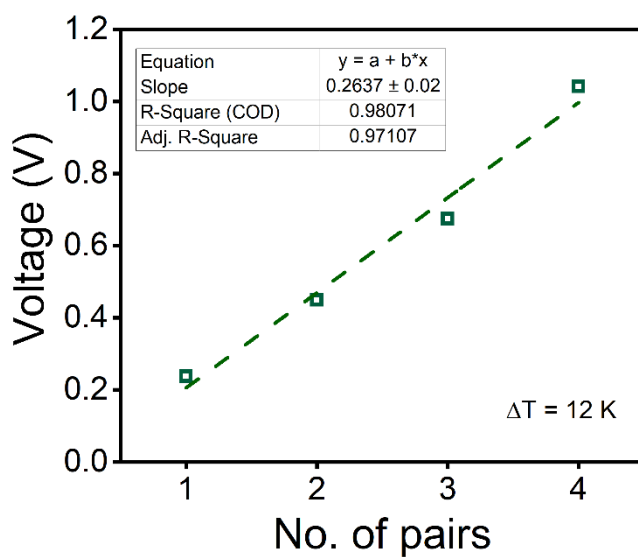


Figure S21: Increment of thermovoltages with the increase of pairs of Ni-PSS-M and Ni-AC-Cl-M-29 3.9 thermopiles.

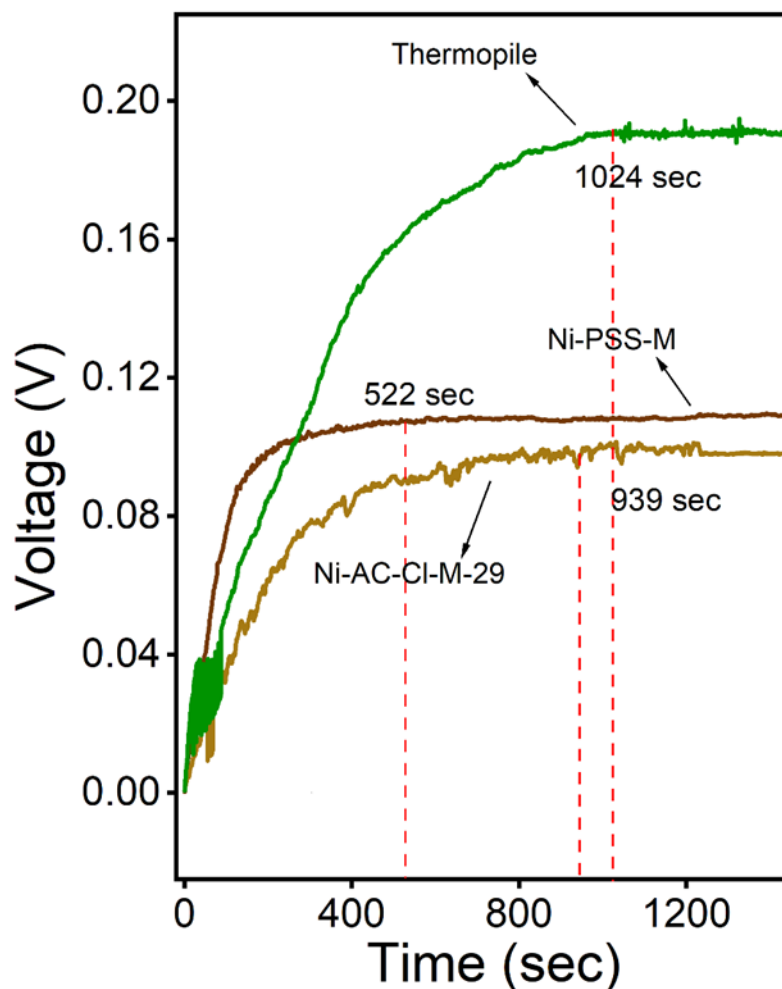


Figure S22: Different saturation time to attain the saturation voltage for Ni-AC-Cl-M-29, Ni-PSS-M and the thermopile composed of these two membranes.

References:

- 1 K. Saha, J. Deka, R. K. Gogoi, K. K. R. Datta and K. Raidongia, *ACS Appl. Nano Mater.*, 2022, **5**, 15972–15999.
- 2 J. Deka, K. Saha, R. Gogoi, G. K. Dutta and K. Raidongia, *ACS Appl. Electron. Mater.*, 2021, **3**, 277–284.
- 3 Z. A. Akbar, J.-W. Jeon and S.-Y. Jang, *Energy Environ. Sci.*, 2020, **13**, 2915–2923.
- 4 H. Wang, D. Zhao, Z. U. Khan, S. Puzinas, M. P. Jonsson, M. Berggren and X. Crispin, *Adv. Electron. Mater.*, 2017, **3**, 1700013.